Disorder, oscillatory dynamics and state switching: the role of c-Myc

Nivedita Rangarajan [a], Zach Fox [b], Abhyudai Singh [b,c], Prakash Kulkarni [d,*], Govindan Rangarajan [e,f,**]

[a] Indian Institute of Science Education and Research, Pune, India
[b] Biomedical Engineering, University of Delaware, Newark, DE, USA
[c] Electrical and Computer Engineering, University of Delaware, Newark, DE, USA
[d] Department of Urology and Oncology, The Johns Hopkins University School of Medicine, Baltimore, MD, USA
[e] Department of Mathematics, Indian Institute of Science, Bangalore, India
[f] Centre for Neuroscience, Indian Institute of Science, Bangalore, India

HIGHLIGHTS

- A Myc threshold plays a critical role in determining cell fate.
- Below the Myc threshold, phenotype is normal but above it, Myc switches states.
- It inactivates p53/Mdm2 oscillator; pushes cyclin/cdk2 oscillator into overdrive.
- When downregulated, Myc inactivates cyclin/cdk2 oscillator and reverses phenotypes.
- A feedback loop coupled with Myc sequestration generates bistable Myc levels.

ARTICLE INFO

ABSTRACT

In this paper, using the intrinsically disordered oncoprotein Myc as an example, we present a mathematical model to help explain how protein oscillatory dynamics can influence state switching. Earlier studies have demonstrated that, while Myc overexpression can facilitate state switching and transform a normal cell into a cancer phenotype, its downregulation can reverse state-switching. A fundamental aspect of the model is that a Myc threshold determines cell fate in cells expressing p53. We demonstrate that a non-cooperative positive feedback loop coupled with Myc sequestration at multiple binding sites can generate bistable Myc levels. Normal quiescent cells with Myc levels below the threshold can respond to mitogenic signals to activate the cyclin/cdk oscillator for limited cell divisions but the p53/Mdm2 oscillator remains nonfunctional. In response to stress, the p53/Mdm2 oscillator is activated in pulses that are critical to DNA repair. But if stress causes Myc levels to cross the threshold, Myc inactivates the p53/Mdm2 oscillator, abrogates p53 pulses, and pushes the cyclin/cdk oscillator into overdrive sustaining unchecked proliferation seen in cancer. However, if Myc is downregulated, the cyclin/cdk oscillator is inactivated and the p53/Mdm2 oscillator is reset and the cancer phenotype is reversed.

© 2015 Elsevier Ltd. All rights reserved.

1. Introduction

The oncogene, c-Myc, (henceforth referred to as just Myc) is implicated in the regulation of a wide variety of biological processes including control of cell division, growth, differentiation, apoptosis, and angiogenesis (Marcu et al., 1992). The protein belongs to the class of basic-helix–loop–helix–leucine zipper transcription factors that can heterodimerize with other members in this class and bind to a canonical DNA sequence, the E-box, to regulate the expression of target genes (Facchini and Penn, 1998). Thus, it is generally held that Myc orchestrates the efficient and orderly proliferation of normal cells by modulating expression of an ever-increasing number of Myc-specific target genes in a dose- and context-dependent manner (Shaffer et al., 2006; Margolin et al., 2009; Wasylishen and Penn, 2010; Ji et al., 2011). However, Myc can also cause a wide variety of cells to switch states from a differentiated, non-dividing state to an oncogenic, proliferative one by attenuating the intrinsic tumor suppressor pathways which ensure that the damaged cell is either repaired or cannot

* Correspondence to: Institute for Bioscience & Biotechnology Research, University of Maryland, 9600 Gudelsky Drive, Rockville, MD 20850, USA.
** Corresponding author at: Department of Mathematics, Indian Institute of Science, Bangalore 560012, India. Tel.: +91 80 2360 0373; fax: +91 80 2360 0146.
E-mail addresses: pkulkar4@ibbr.umd.edu (P. Kulkarni), rangaraj@math.iisc.ernet.in (G. Rangarajan).

propagate (Felsher et al., 2000; Shachaf et al., 2004). But how cells discriminate between normal and oncogenic Myc signaling, is a puzzling question.

On the other hand, in conjunction with the embryonic transcription factors Oct4, Sox2 and Nanog, Myc facilitates the reprogramming of somatic cells to pluripotent stem cells *in vitro* (Takahashi and Yamanaka, 2006). Furthermore, since Myc is overexpressed in many cancers (Cole and Henriksson, 2006; Huang et al., 2014), a potential relationship between cancer and the embryonic stem (ES) cell states has long been suspected. However, a comparison of ES cells to metastatic cancer cells that are believed to exhibit stem cell-like properties (Ben-Porath et al., 2008; Kim and Orkin, 2011) (the so-called cancer stem cells or CSCs) revealed that only Myc, but not the other genes that are expressed in ES cells, is upregulated in both cell types suggesting that CSCs may share only one or few of the ES cell characteristics (Kim et al., 2010). Nonetheless, these results further reinforce the notion that different cellular states are defined by gene expression signatures characteristic of that state and that, Myc is an important contributor to the state-specific gene expression.

But contrary to the prevailing wisdom, recent observations have revealed that forced overexpression of Myc causes a linear amplification of only those genes that are actively engaged in transcription by Myc and that, the protein does not instruct gene expression *de novo* (Lin et al., 2012; Nie et al., 2012). Furthermore, consistent with an earlier observation regarding transcriptional pause release (Rahl et al., 2010), it was concluded that Myc may act to alleviate pausing of RNA polymerases poised on all active genes in a given cell type (Lin et al., 2012; Nie et al., 2012). Thus, an important question that remains poorly understood is if Myc merely reinforces its pre-existing transcriptional program and hence, the phenotypic state, how does Myc expression direct normal somatic cell proliferation on the one hand and cause it to switch states from normal to malignant or from a differentiated to a pluripotent state on the other?

Further, cancer caused by Myc overexpression, albeit early-stage disease in an animal model, appears to be reversible (Shachaf et al., 2004; Felsher and Bishop, 1999). Thus, while overexpression of Myc induced liver cancer in a transgenic mouse model that was accompanied by extensive genetic alterations in the transformed cells, switching Myc off in these cells reversed the tumorigenic process and returned the cells to normalcy despite the genetic alterations. However, turning Myc on again resulted in the dormant cells redeveloping cancer. Remarkably, the authors confirmed that the genomic alterations that had occurred in the cancer cells overproducing Myc remained unchanged when the Myc-expressing cells cycled between the cancerous and "normal" states (Shachaf et al., 2004). It is generally held that mutations drive tumorigenesis (Vogelstein and Kinzler, 2004; Stratton et al., 2009); if so, how can dialing down Myc expression reverse the process albeit, in the early stages?

Therefore, in light of the fact that cancer cells, like all other living and many non-living systems, are self-organizing systems, we reasoned that perhaps a dynamical systems approach could help shed new light on how Myc enables cells to switch states and specify cell fate. Indeed, such an approach has been quite successful in providing new insight regarding the molecular mechanisms underlying state switching by ES cells to form stably differentiated lineages (Kalmar et al., 2009; Glauche et al., 2010; Chickarmane et al., 2012). Furthermore, while there have been several reports modeling the interactions between the p53 oscillator and cell cycle (Alam et al., 2015; Sun et al., 2011), the role of positive/negative feedback loops in generating p53 oscillations (Ciliberto et al., 2005; Kim and Jackson, 2013), and the role of p53 oscillations in cell fate decision (Purvis et al., 2012), the role of Myc

in modulating cellular oscillatory dynamics has not been explored to the best of our knowledge.

Using cancer as an example, we show that by modeling varying levels of Myc overexpression, one could switch cellular states from a cancer phenotype to a normal phenotype. Toward this end, we demonstrate how fluctuations in Myc levels can cause bistability and hysteresis and using deterministic oscillator models, illustrate how the "high" and "low" levels (on/off levels, respectively) of Myc can affect the coupling constants and hence, the dynamics of key oscillators to impact cellular decision making.

2. Mathematical models of oscillators

We begin by briefly describe two key modules of the Myc network namely, the p53/Mdm2 oscillator and the cyclin/cdk2 oscillator (Fig. 1), and their corresponding mathematical models.

2.1. The p53/Mdm2 oscillator

The protein p53, a tumor suppressor which is activated in response to stress, is a key regulator of a range of processes involved in tumorigenesis, including cell cycle arrest, DNA repair, and apoptosis (Vousden and Lane, 2007; Aylon and Oren, 2007). The protein is a transcription factor (Kern et al., 1991) that is activated upon phosphorylation by Ataxia telangiectasia mutated (ATM), a serine/threonine protein kinase. ATM is recruited and activated by DNA double-strand breaks and phosphorylates several key proteins that initiate activation of the DNA damage checkpoint, leading to cell cycle arrest, DNA repair or apoptosis (Shiloh, 2006; Lee and Paull, 2007). ATM directly interacts with the MRN complex and phosphorylates the histone variant H2AX. This phosphorylation generates binding sites for adapter proteins that then recruit the effector protein kinase CHK2 and the tumor suppressor p53 (Lee and Paull, 2007). Activated p53 binds DNA and upregulates the expression of several genes including micro-RNA miR-34a, WAF1/CIP1 encoding for p21. The protein p21 binds to the G1-S/CDK (cell cycle-dependent kinases namely, cdk2) and S/CDK complexes that are important for the G1/S transition in the cell cycle and inhibits their activity and thus serves as an important checkpoint component. The expression of p21 is regulated by p53, through which this protein mediates the p53-dependent cell cycle G_1 phase arrest in response to a variety of stress stimuli.

In unstressed cells, p53 levels are kept low through a continuous degradation process. The murine double minute 2 (Mdm2, HDM2 in humans), whose transcription is directly regulated by p53, binds to p53, preventing its action and transports it from the
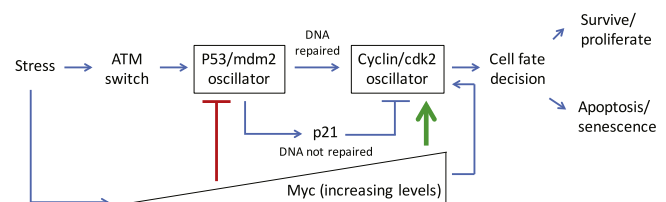

Fig. 1. Increasing Myc expression can cause state/phenotypic switching in absence of differential gene expression and/or genetic alterations. In this scenario, cancer is a case of state/phenotype switching from a normal to a malignant phenotype. A fundamental assumption of the model is that a Myc threshold determines cell fate. When a normal cell experiences stress, ATM is activated that in turn activates p53 by phosphorylating it. As a result, Mdm2 disassociates from p53 and p53 activates the DNA repair pathway. If the DNA is repaired, the cell makes the decision to survive. On the other hand, if the damage is beyond repair, the cell decides to commit apoptosis. However, if the oncogene Myc is upregulated due to stress and exceeds the critical threshold, it kills the p53/Mdm2 oscillator but activates the cyclin E/cdk2 oscillator and the cell overrides the apoptosis pathway to initiate unchecked proliferation.

nucleus to the cytosol. Also Mdm2 acts as ubiquitin ligase and covalently attaches ubiquitin to p53 and thus marks p53 for degradation by the proteasome forming a negative feedback loop. Together, the positive and negative feedback loops between p53 and Mdm2 are responsible for robust oscillatory dynamics (Iwakuma and Lozano, 2003).

Previously, it was believed that p53 responds to DNA damage in an analog mode that is, low levels of p53 would ensure cell survival by facilitating cell cycle arrest and DNA repair, while higher levels would ensure genome integrity and cause apoptosis (Vousden and Lane, 2007). However, recent studies have revealed that the feedback loop is delayed and combines with the ATM-controlled feedback strength and effective dampening of the negative feedback loop to produce limit-cycle oscillations (Wagner et al., 2005). Furthermore, studies at the single cell level by Lahav et al. (2004) have revealed that activated ATM initiates the p53 oscillator to produce a series of discrete pulses after DNA damage. Genetically identical cells had different numbers of pulses (zero, one, two or more) but the mean height and duration of each pulse were fixed and were not dependent on the amount of DNA damage. However, there was good correlation between the mean number of pulses and DNA damage (Lahav et al., 2004). Based on these and other observations, Zhang et al. (2009) developed a theoretical model to explain how p53 pulses may determine cell fate. Their model showed that, at low damage levels, few p53 pulses evoke cell cycle arrest by inducing p21 and promote cell survival, whereas at high damage levels, sustained p53 pulses trigger apoptosis by inducing p53 AIP1 (Zhang et al., 2009; Batchelor et al., 2008).

2.2. The p53/Mdm2 oscillator model

This and the subsequent models are based on the assumption that there is a critical threshold of Myc levels in the cell and the central tenet of the model is that Myc, when upregulated beyond a critical threshold functions as an oncogene to cause cancer. It is important to note that this is not a tacit assumption and in fact, experimental observations have revealed that there is a precise threshold level of Myc expression that is required for maintaining the cancer phenotype (Shachaf et al., 2008). However, Myc is negatively regulated by the tumor suppressor p53 (Sachdeva et al., 2009; Levy et al., 1993; Ho et al., 2005). Thus, there is a balance of power in the cell with regard to these two opposing forces that determine cell fate. Therefore, we posit that for Myc to exert its oncogenic potential, it would have to override the p53 checkpoint by inactivating the p53/Mdm2 oscillator and engage the cyclin/cdk2 oscillator in overdrive to sustain unchecked proliferation seen in cancer. However, in our model, we do not consider the various post translational modifications that could affect Myc activity (Wang et al., 2011; Cao et al., 2011). Finally, all non-linearities in the model are of the Michaelian type in that, no form of cooperativity is assumed.

For the p53–Mdm2 oscillator, we take the deterministic version of model IV considered in Geva-Zatorsky et al. (2006) (this model has again been fitted to experimental data and is for a somatic cell)

$$\frac{dy_1}{dt} = \beta_x - \alpha_x y_1 - \alpha_k y_3 \frac{y_1}{k + y_1} \tag{1}$$

$$\frac{dy_2}{dt} = \beta_y y_1 - \alpha_0 y_2 \tag{2}$$

$$\frac{dy_3}{dt} = \alpha_0 y_2 - \alpha_y y_3 \tag{3}$$

Here y_1, y_2 and y_3 denote the concentrations of nuclear p53, Mdm2 precursor and nuclear Mdm2 respectively the details for

which are described by Geva-Zatorsky et al. (2006). Again, we assume that Myc levels, when they cross a critical threshold, control the Michaelis constant k. Here sub-threshold Myc levels correspond to low values of k while high Myc values correspond to high values of k. This model that is based on a feedback regulation, of p53 by ATM and Mdm2 respectively, or the phosphorylation–dephosphorylation of cdk2, follows the Michaelian nature of the product decay term that has been demonstrated to markedly influence the period, amplitude, and waveform of the oscillations (Fall et al., 2002).

2.3. The cyclin/cdk oscillator

Cyclins and the cyclin-dependent kinases (cdks) are two key classes of regulatory molecules that determine a cell's progress through the cell cycle (Evans et al., 1983). The two classes of molecules interact to form specific heterodimers and while cyclins form the regulatory subunits, the cdks form the catalytic subunits of the activated heterodimer. As cyclin progressively increases beyond a threshold, it causes the activation of cdk with which it forms a heterodimeric complex called mitosis-promoting factor (MPF). MPF triggers mitosis as well as cyclin degradation (Maller et al., 1989). Subsequent inactivation of the cdk resets the cell for a new division cycle. Although, the mechanism involves additional checkpoints in mammalian cells they also rely on the periodic activation of cdk that is achieved by reversible covalent modification. Activation of cdk before the onset of mitosis involves its dephosphorylation, whereas the enzyme is inactivated after mitosis through rephosphorylation (reviewed (Johnson and Walker, 1999)).

The various cyclins and cdks form a network that is sequentially activated and is regulated by intertwined negative and positive feedback loops. This network is capable of temporal self-organization in the form of sustained oscillations that govern the ordered progression through the successive phases of the cell cycle. When activated by binding to cyclin, the cdks phosphorylate target proteins to orchestrate entry into the next phase of the cell cycle. Thus, the cyclin–cdk system can operate as a continuous autonomous oscillator (Goldbeter, 1991; Csikasz-Nagy et al., 2006). However, since the cdk molecules are always present in excess, the availability of the cyclins determines the concentration of the active cyclin/cdk complex. Furthermore, the availability of this complex is subject to several regulatory mechanisms including phosphorylation and degradation by APC/cdc (Csikasz-Nagy et al., 2006). Although, different cyclin–cdk combinations determine downstream protein targets, cyclin E activates cdk2 to push the cell from G1 to S phase which initiates the G2/M transition. Of particular note, p53 regulates the expression of p21 (aka CDKN1), which interacts with cdk2. When p21 is complexed with cdk2, the cell cannot continue to the next step of cell division.

2.4. The cyclin/cdk oscillator model

We begin with a detailed and physiologically realistic mathematical model that governs the mammalian somatic cell cycle that includes the gap phases as described by Csikasz-Nagy et al. (2006). This model involves 13 ordinary differential equations, 21 other defining equations and 74 kinetic rate constants and has been benchmarked against experimental results (Weis et al., 2014). The explicit equations and parameter values are not described here because of the complexity but can be found on the website http://igcell.cs.vt.edu/generic_model/GenericUC.php

The parameter of interest to us is the Michaelis constant J_{a20}. The equation that it appears in (Csikasz-Nagy et al., 2006) is

reproduced below

$$\frac{dCdc20_A}{dt} = \frac{k_{a20} \cdot APC \cdot (Cdc20_T - Cdc20_A)}{J_{a20} + Cdc20_T - Cdc20_A}$$
$$- \left(\frac{k_{i20}}{J_{i20} + Cdc20_A} + k_{d20} \right) \cdot Cdc20_A \qquad (4)$$

It is clear that J_{a20} is involved in the APC (anaphase promoting complex) dependent synthesis of $Cdc20_A$. Further details regarding this and the other parameters can be found in Csikasz-Nagy et al. (2006). Further, we assume that Myc levels control the Michaelis constant J_{a20}. Myc levels below a critical threshold (found in normal cells) give rise to high values of J_{a20} and overexpression of Myc above the threshold (characteristic of cancer cells) leads to low values of J_{a20}.

2.5. General oscillator model

It is well known that biological systems in the form of chemical reaction networks display non-trivial qualitative behaviors such as switching and chaotic dynamics in addition to oscillation (Fall et al., 2002; Goldbeter et al., 2001). Thus, one concern in modeling biological systems is in understanding the scope of behaviors that the model can elicit. Furthermore, the parameter space is often quite large in such systems and therefore, identifying potentially interesting dynamics in this space can be difficult. However, the onset of qualitative changes in the parameter space occurs at specific points, the Hopf bifurcation points, which mark the transition between oscillatory and non-oscillatory behavior characterized by particular changes in the eigenvalues that describe the local dynamics of the model. Therefore, we will concentrate on the system's behavior in the neighborhood of such bifurcation points.

But in theoretical studies, often times, the applicability or validity of a particular model can also be a matter of concern. It is therefore important to demonstrate that the transition for oscillatory to non-oscillatory behavior (or vise versa) can also occur in generic coupled oscillators. Thus, in addition to the specific models described above, we also consider a generic mathematical model for coupled oscillators. We start with a very general form of a nonlinear oscillator

$$\frac{dz_1}{dt} = f_1(z_1, z_2, p) \qquad (5)$$

$$\frac{dz_2}{dt} = f_2(z_1, z_2, p) \qquad (6)$$

Here z_1, z_2 are coordinates describing the ith oscillator, f_i is a nonlinear function (with the Jacobian of the system required to have complex conjugate eigenvalues since it describes an oscillator) and p is a system parameter. By linearly coupling two such oscillators together and linearizing around the equilibrium solution, Aronson et al. (1987) have rigorously demonstrated that a canonical mathematical model can be obtained for two linearly coupled oscillators.

Consequently, close to the Hopf bifurcation point p_0 and by restricting to diffusive coupling for simplicity, we obtain the following canonical Stuart–Landau coupled oscillator model (Aronson et al., 1987; Kuramoto, 1984) in polar coordinates

$$\frac{dr_i}{dt} = (a_i - r_i^2 - KA_{12})r_i + K \sum_{k=1}^{2} A_{ik} r_k \, \cos(\theta_k - \theta_i) \qquad (7)$$

$$\frac{d\theta_i}{dt} = \omega_i + K \sum_{k=1}^{2} A_{ik} \frac{r_k}{r_i} \, \sin(\theta_k - \theta_i) \qquad (8)$$

Here $i = 1, 2$, $r_i^2 = (x_i^2 + y_i^2)$, $\theta_i = \tan^{-1}(y_i/x_i)$, a_i are the growth rates, K is the coupling constant, $A_{11} = A_{22} = 0$, and $A_{12} = A_{21} = 1$.

Note that x_i and y_i denote deviations from steady state concentrations in our context and hence can take negative values when they oscillate. In this generic model, we hypothesize that different Myc values change the value of coupling constant K. It should be noted that even the Michaelis constant J_{a20} in the previous cyclin–cdk2 cascade model or the Michaelis constant k in the p53–Mdm2 oscillator model can be thought of as an effective coupling constant in the following manner. For example, in Eq. (1), we can pull out the Michaelis constant k from the denominator and the right hand side of the equation can be rewritten as $\beta_x - \alpha_x y_1 - \alpha_k \frac{y_3}{k} \frac{y_1}{1 + y_1/k}$. Hence, $1/k$ can be thought of as a coupling constant that couples y_1 and y_3. Therefore, in every case, the essential hypothesis is that different Myc levels correspond to different values of the appropriate coupling constant. It should be noted that the above generic oscillator model can be extended to an arbitrary number of nonlinear systems coupled to one another. However, we have restricted ourselves to two systems for simplicity.

3. Results

3.1. Excursions in Myc levels can influence the oscillatory dynamics of key cellular oscillators

Using different oscillator models, we demonstrate how Myc expression might trigger state switching by assuming that, beyond a given threshold, Myc changes a key coupling constant that regulates the p53/Mdm2 and cyclin/cdk2 oscillators. In this scenario, we envision cancer as a case of state/phenotype switching from a normal to a malignant phenotype through a (inverse) Hopf bifurcation where the functional p53/Mdm2 oscillator is inactivated and the cyclin/cdk2 oscillator is activated for sustained, unchecked proliferation. This scenario is schematically illustrated in Fig. 2.

First, we numerically simulate the mammalian cell cycle model using XPP (http://www.math.pitt.edu/~bard/xpp/xpp.html). We hypothesize that Myc downregulation corresponds to values of the constant J_{a20} greater than K^*, the bifurcation point (Fig. 2). The
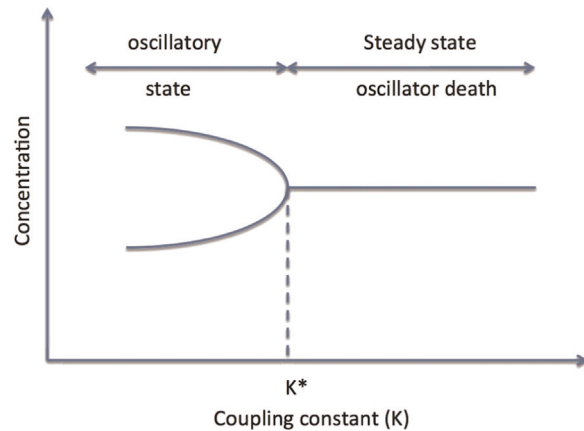
Fig. 2. This figure illustrates the general scenario where different Myc levels can give rise to different states. As the coupling constant K increases, the system undergoes a bifurcation at the value K^*. Here K is a generic coupling constant. For a specific system, K will be identified with one of the constants of the system. For $K < K^*$, the system exhibits oscillations where the 2 lines denote the minimum and maximum values of the oscillations. For $K > K^*$, the system exhibits a non-oscillatory steady state (oscillator death). In the cyclin/cdk2 system, we hypothesize that when the Myc concentration is below a critical threshold, K is greater than K^* (for this system K is identified with J_{a20}). When the Myc concentration goes above this threshold, K is less than K^*. In the p53/Mdm2 system, on the other hand, Myc concentration below a threshold is hypothesized to correspond to $K < K^*$ and Myc concentration above this threshold corresponds to $K > K^*$ (for this system K is identified with k).
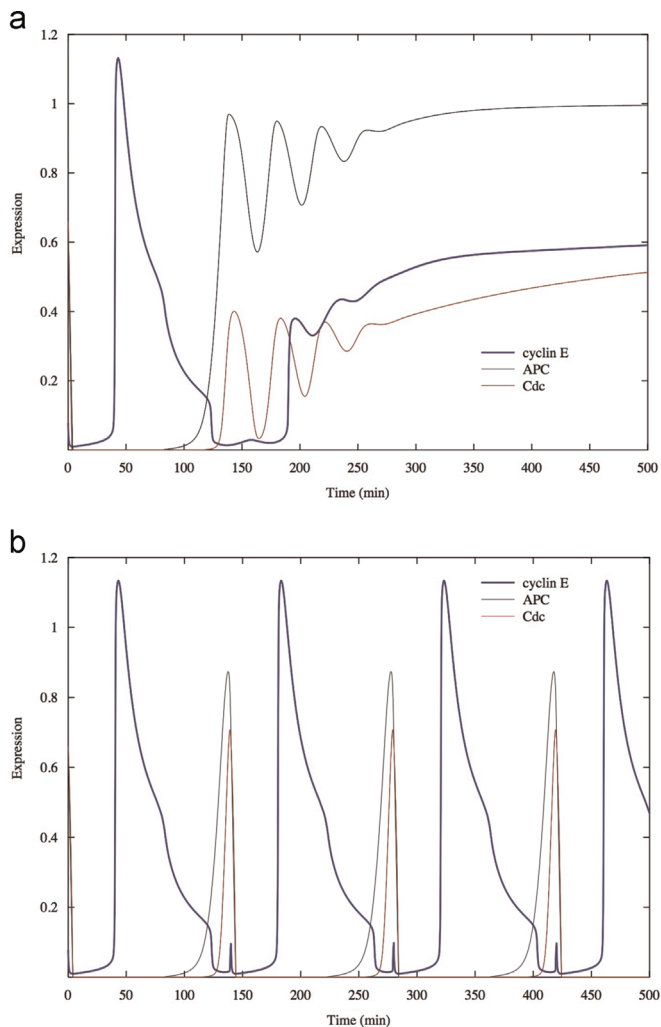
a

b

Fig. 3. State switching in cyclin/cdk2 system between steady state and oscillatory state. APC is the anaphase promoting complex and cell division cycle (cdc) is the highly conserved activator of APC. Together they promote cell-cycle-regulated ubiquitination and proteolysis of a number of critical cell cycle-regulatory targets. Note, here cyclin E represents the cyclin in the cyclin/cdk2 complex in mammals (Csikasz-Nagy et al., 2006). (A) Cyclin/cdk2 cascade for $J_{a20} = 0.2$ (Myc value below threshold). System is in a steady state and no oscillations are present. The other parameter values used are the same as those given on the website http://jigcell.cs.vt.edu/generic_model/GenericUC.php (B) cyclin/cdk2 cascade for $J_{a20} = 0.005$ (Myc value above threshold). System switches to an oscillatory state. Other parameter values are the same as in (A).
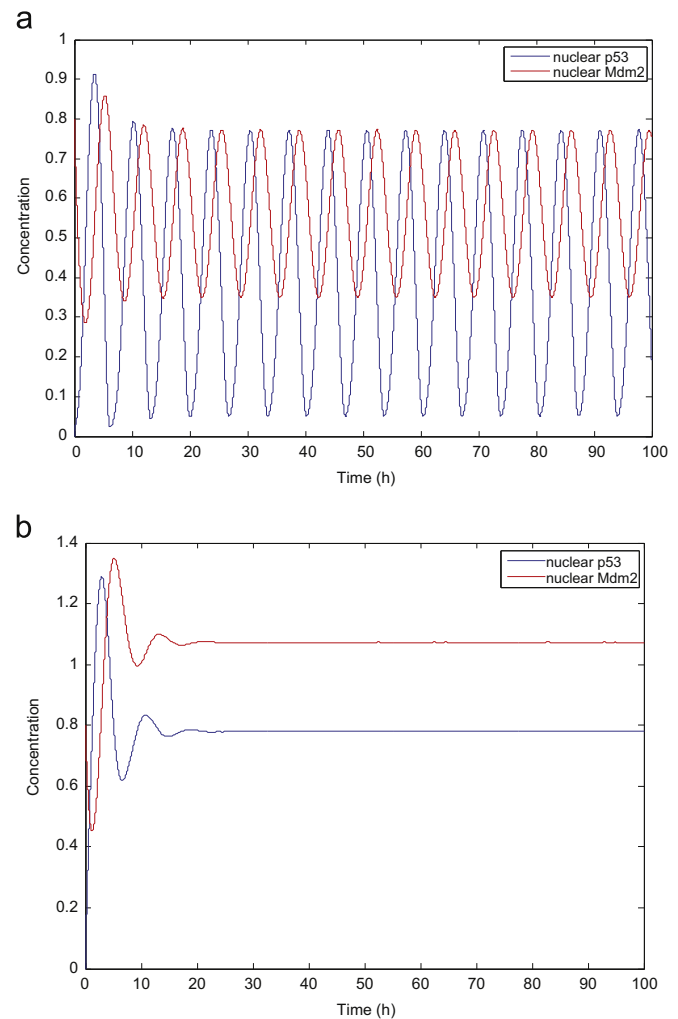
a

b

Fig. 4. State switching in p53–Mdm2 system between oscillatory and steady states. (A) System is in an oscillatory state for $k=0.01$ (Myc value below threshold). The other parameter values used are given in the Matlab code in the Supplementary file. (B) System switches to a steady state for $k=0.8$ (Myc value above threshold). The other parameter values are the same as in (A).

results obtained for $J_{a20} = 0.2$ is shown in Fig. 3A. We see that there are no oscillations of cyclin and cdk2 in this case and hence this corresponds to a differentiated healthy cell. On the other hand, if Myc is upregulated and consequently J_{a20} is small (0.005), we obtain oscillations in cyclin and cdk2 (Fig. 3B). This corresponds to an increase in the proportion of cells that are in active cell division (versus quiescent cells in G0 phase) in cancer compared to normal tissue. There is thus a net increase in cell number, as the number of cells that die by apoptosis or undergo senescence remains the same. The above results are robust against changes in parameter values.

We obtain similar results for the p53–Mdm2 oscillator using ode45 Matlab routine (MATLAB version 7.12. Natick, Massachusetts: The MathWorks Inc., 2011). The Matlab code is given in the Supplementary file. For low Myc values, we take k to be below the bifurcation point (Fig. 2). In this case, taking k to be 0.01, we obtain oscillations in the p53 and Mdm2 concentrations (Fig. 4A).

Oscillations in p53 concentrations are known to lead to repair of damaged DNA. If Myc is upregulated, k values are taken to be greater than the bifurcation point. Taking k to be 0.8, we obtain oscillator death in this case (that is, p53 concentrations no longer oscillate) (see Fig. 4B). Therefore, the DNA repair pathway is disabled in cancer with inactivated p53/Mdm2 oscillator. Again, the above results are robust against changes in parameter values.

Finally, to demonstrate that such results are not model dependent, we next simulate two coupled Stuart–Landau oscillators (Matlab code is given in the Supplementary file). Here we hypothesize that low Myc levels correspond to values of the coupling constant K above the bifurcation point. For $K = 1.4$, we obtain zero values for the deviations of concentrations around the steady state value (Fig. 5A). This is a well-known phenomenon in nonlinear dynamics (Aronson et al., 1990). On the other hand for $K = 0.5$ (below the bifurcation point and corresponding to Myc values greater than the threshold), we get oscillations in the concentrations (Fig. 5B). Therefore, even in a generic model of coupled oscillators, we find the transition between oscillatory and non-oscillatory state depending on the coupling constant (whose value, we hypothesize, depends on the Myc concentrations).
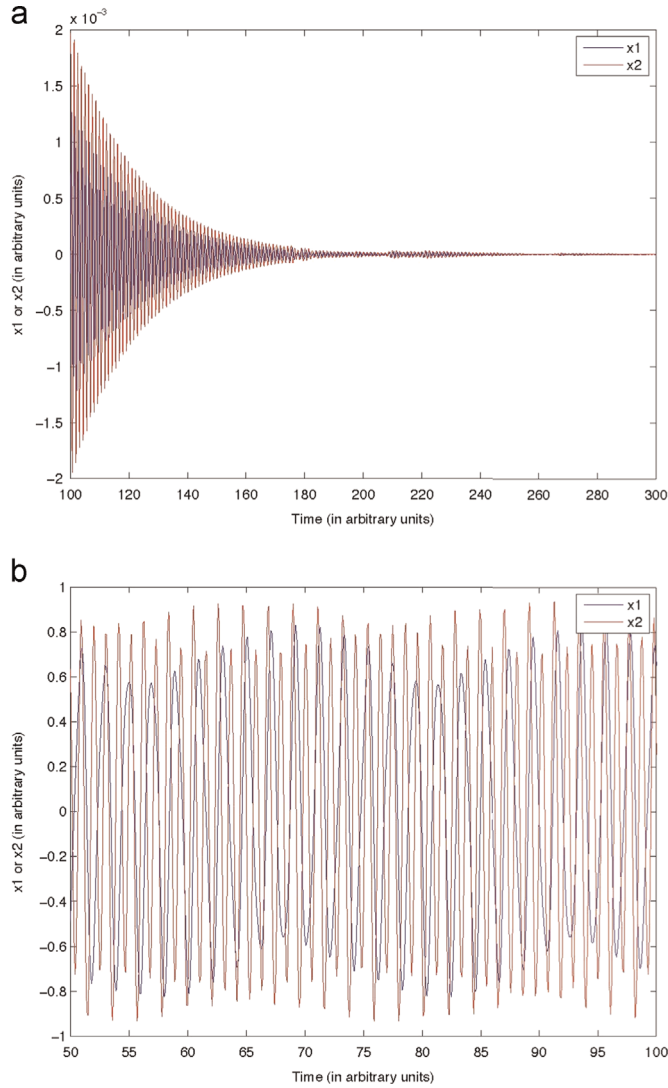
a

b

Fig. 5. State switching in a generic Stuart–Landau system between steady state and oscillatory state. (A) System is in a steady state and no oscillations are present for $K = 1.4$ (Myc value below threshold). The other parameter values used are: $a_1 = 1.0$, $a_2 = 1.2$, $\omega_1 = 3.0$, $\omega_2 = 6.0$. (B) System switches to an oscillatory state for $K = 0.5$ (Myc value above threshold). The other parameter values are the same as in (A).

3.2. Bistability and hysteresis in the Myc interaction network

In the present study, it is implicit that there is significant fluctuation in Myc levels to satisfy the key assumption that a Myc threshold determines cell fate of cells in which p53 is expressed. Indeed, recent studies have shown that, both the Myc transcript as well as Myc protein level are subject to multiple feedback systems resulting in huge fluctuations in the temporal distribution of Myc. For example, there exists a positive feedback loop between Myc and Sirtuin 1 (SIRT1) (Menssen et al., 2012; Marshall et al., 2011). Myc up regulates SIRT1 expression, and SIRT1 in turn increases Myc stability. Similarly, another study has found a positive feedback between Myc and ENBA1 binding protein 2 (EBP2): Myc activates EBP2 by directly binding to its promoter, and EBP2 blocks Myc degradation (Liao et al., 2014). Not surprisingly, both Myc and EBP2 are upregulated in cancerous tissues (Liao et al., 2014). Therefore, we asked if such feedbacks are sufficient to generate bistability in the system since bistability could provide a mechanism by which sharp transitions can occur between low-Myc and high-Myc states. Furthermore, it is important to note that Myc, being an intrinsically disordered protein (IDP), binds to a
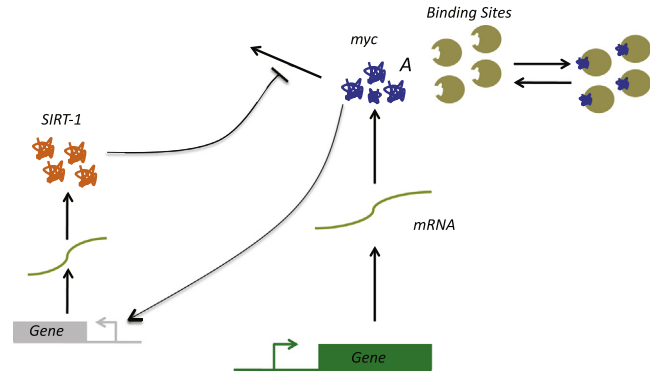

Fig. 6. Schematic of the Myc interaction network. Myc up regulates expression of SIRT1, which in turn increases Myc protein stability creating a positive feedback circuit (Evans et al., 1983; Maller et al., 1989). Myc being an intrinsically disordered protein (IDP), binds to a broad range of sites on DNA and partner proteins. These sites function to sequester Myc away from activating SIRT1.

multitude of binding sites on DNA and partner proteins. This sequestration of Myc is an important component in the bistability, as we shall see below. Thus the IDP nature of Myc plays a crucial role in our model.

Using ordinary differential equations (ODE) we model the Myc–SIRT1 positive feedback loop together with Myc sequestration at binding sites. A schematic of the Myc–SIRT1 regulatory system is illustrated in Fig. 6. We represent by N the total number of Myc binding sites in the cell. The Myc protein binds and unbinds to these sites with rates k_b and k_u, respectively. Myc mRNA is transcribed at a rate k_m and degrades with rate γ_m. Protein molecules are translated from each mRNA at a rate k_p. Let $m(t)$, $x(t)$ and $x_f(t)$ denote the concentrations of Myc mRNA, total (bound and unbound) Myc, and free (unbound) Myc protein, respectively, at time t inside the cell. As discussed earlier, SIRT1 enhances Myc protein stability. Assuming SIRT1 levels are proportional to x_f (SIRT1 is activated by free Myc), a non-cooperative positive feedback loop is incorporated in the system by setting the Myc degradation rate as

$$\gamma_x \left(1 + \frac{k_1 - 1}{1 + cx_f}\right), \tag{9}$$

which gradually decreases with increasing x_f. With this formulation, degradation rate is γ_x and $k_1\gamma_x$, when Myc levels are high and low, respectively. Thus, $k_1 > 1$ is the fold-change in Myc stability. Constant c defines the concentration $x_f = 1/c$ at which point Myc degradation rate is roughly half of its maximum value. Based on this model description, we obtain the following set of differential equations describing the time evolution of $m(t)$, $x(t)$ and $x_f(t)$

$$\frac{dm}{dt} = k_m - \gamma_m m, \tag{10}$$

$$\frac{dx_f}{dt} = k_p m - \gamma_x \left(1 + \frac{k_1 - 1}{1 + cx_f}\right)x_f - k_b x_f (N - (x - x_f)) + k_u(x - x_f), \tag{11}$$

$$\frac{dx}{dt} = k_p m - \gamma_x \left(1 + \frac{k_1 - 1}{1 + cx_f}\right)x. \tag{12}$$

Note that $N - (x - x_f)$ and $(x - x_f)$ are the levels of unbound binding sites and bound Myc, respectively. Hence, the terms $k_b x_f (N - (x - x_f))$ and $k_u(x - x_f)$ in Eq. (11) represent the loss and gain of free Myc due to the unbinding/binding process.

We assume that Myc binding and unbinding occurs at a much faster time scale than Myc production and degradation. A quasi steady-state approximation for the fast reactions yields

$$k_b \bar{x}_f (N - (\bar{x} - \bar{x}_f)) = k_u(\bar{x} - \bar{x}_f), \tag{13}$$

where $\bar{x}_f$ and $\bar{x}$ are the steady-state values of free and total Myc,
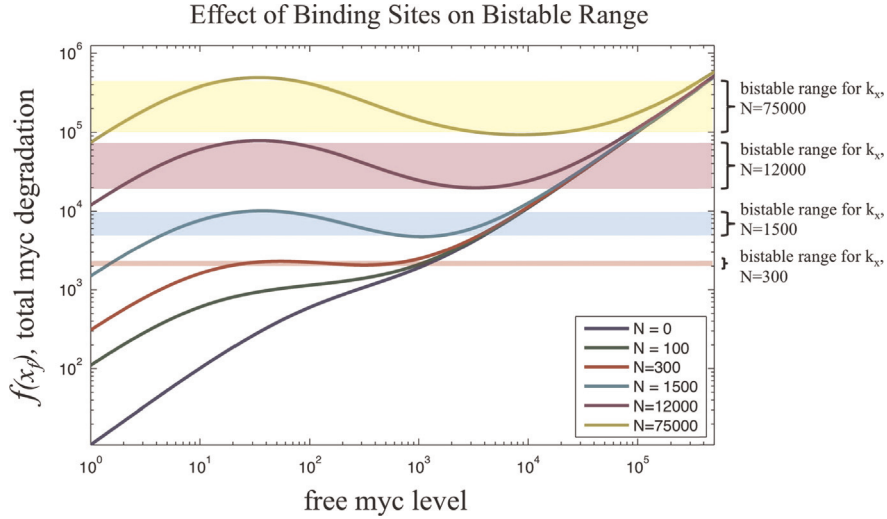
Fig. 7. Non-cooperative positive feedback loop together with Myc sequestration generates bistability. Plot of the total Myc degradation rate f (right-hand-side of Eq. (15)) as a function of the free Myc level. When $N=0$ (i.e., no Myc binding sites), f increases monotonically and there is always a unique stable Myc equilibrium for any given production rate k_x (left-hand-side of Eq. (15)). However, for large values of N, f is non-monotonic with two stable Myc equilibriums possible for a range of production rates. Range of k_x values that generate bistability increases with N. Parameters chosen as $k_1=10$, $k_u=10,000$, $k_b=1000$, $c=0.01$. Binding and unbinding rates are normalized to $\gamma_x=1$.
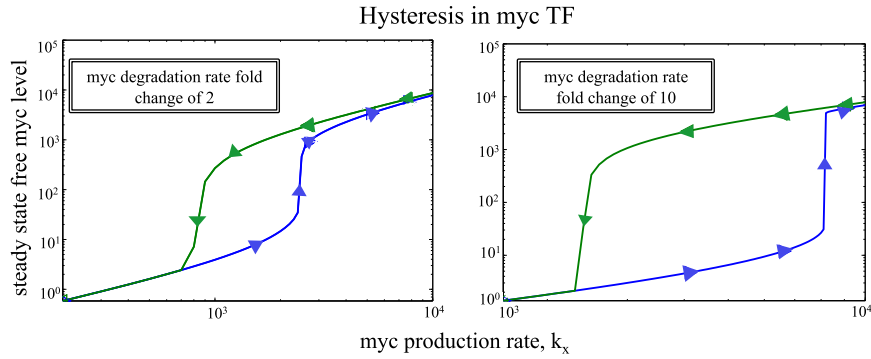

Fig. 8. Bistability and hysteresis in the Myc interaction network. Free Myc levels as a function of the production rate k_x for a two-fold ($k_1=2$; left), and a ten-fold ($k_1=10$; right) change in Myc stability. Bistability arises for a range of production rates in both cases. Initially cells are in a low-Myc state. As production rates increase due to stress, Myc levels gradually build up. Once a critical threshold is crossed, the system transitions to a high-Myc state, and represents the cancerous transformation of the cell. For these plots parameters taken as $N=1200$, $\gamma_x=1$, $k_u=10000$, $k_b=1000$ and $c=0.01$.

respectively. Rearranging terms in Eq. (13)

$$\bar{x} = \bar{x}_f + \frac{k_b \bar{x}_f N}{k_u + k_b \bar{x}_f}. \tag{14}$$

Performing a steady-state analysis of Eqs. (10) and (12), we obtain

$$k_x \equiv \frac{k_m k_p}{\gamma_m} = \gamma_x \left(1 + \frac{k_1 - 1}{1 + c\bar{x}_f}\right)\bar{x} \tag{15}$$

where k_x is referred to as the Myc production rate. Using Eq. (14)

$$k_x = \gamma_x \left(1 + \frac{k_1 - 1}{1 + c\bar{x}_f}\right)\left(\bar{x}_f + \frac{k_b \bar{x}_f N}{k_u + k_b \bar{x}_f}\right) \equiv f(\bar{x}_f) \tag{16}$$

where $f(\bar{x}_f)$ can be interpreted as the total Myc degradation rate. Plots of function $f(\bar{x}_f)$ for different values of N are shown in Fig. 6. In the absence of Myc binding sites ($N=0$), $f(\bar{x}_f)$ increase monotonically, and there exists a unique Myc equilibrium for any given production rate. Thus, non-cooperative feedback by itself is always monostable. However, for large enough N, $f(\bar{x}_f)$ is non-monotonic and generates bistability (Segel and Edelstein-Keshet, 2013) that is, two stable Myc equilibriums, for a range of k_x values (Fig. 7). Analysis of the Eq. (15) reveals that bistability is a robust feature of this system as for any $k_1 > 1$, bistability arises for sufficiently large enough N and c. Fig. 8 exhibits bistability for a two-fold ($k_1=2$) and a ten-fold ($k_1=10$) change in Myc stability.

4. Discussion

Despite intense research efforts, how Myc functions to determine cell fate remains poorly understood. The present work attempts to provide a quantitative perspective on how this important oncogene may drive state switching. The first step is to provide a mechanism for generating bistable Myc levels. Our ODE model demonstrates that a simple non-cooperative positive feedback loop coupled with Myc sequestration at binding sites can generate strong bistability. Intuitively, bistability arises because at low Myc levels, most of the protein is sequestered within binding sites. Due to lack of Myc-mediated SIRT1 activation, Myc is unstable and is contained at low levels. At high Myc levels, enough free Myc is available to activate SIRT1, stabilize Myc protein, and maintain elevated levels of expression. Thus, bistability, due to the SIRT1-mediated feedback and other feedback systems such as specific microRNAs (Aguda et al., 2008; Li et al., 2011), provides a mechanism by which sharp transitions can occur between low-Myc and high-Myc states facilitating state switching.

Having provided a mechanism by which Myc can switch between high and low levels, we assume that these different levels can affect the coupling constants in the various oscillator models leading to transitions between oscillatory and non-oscillatory states. But how might Myc affect the coupling constants, a key

assumption in our model? One plausible mechanism is that since the Myc level is assumed to affect the Michaelis constant, this can be easily achieved by regarding Myc as an inhibitor. Then, from standard chemical kinetics, it follows that such inhibitors can change the Michaelis constant (Ochs, 2014), thus achieving our objective. This could be experimentally verified.

There are other possible indirect mechanisms by which Myc levels could affect the coupling constants. For example, as a transcription factor, Myc regulates the expression of thousands of genes with many encoding proteins that initiate and maintain the transformed state. Experimental evidence indicates that Myc is a direct positive regulator of Mdm2 (Slack et al., 2005) and the microRNA, mir421 (Hu et al., 2010), and a repressor of the cdk inhibitor, p21 (Gartel et al., 2001). Therefore, by modulating the levels of the key checkpoints in cancer, Myc could affect the coupling constants of the cyclin/cdk2 and the p53/Mdm2 oscillators, respectively. For example, the downregulation of ATM via mir421 or p53 itself via Mdm2 could interfere with the number of p53 pulses. The pulsatile response of p53 is important and enables the p53 network to repeatedly evaluate the damage signal and if the damage cannot be repaired before the number of pulses exceeds a critical number, apoptosis results (Zhang et al., 2009). Thus, Myc
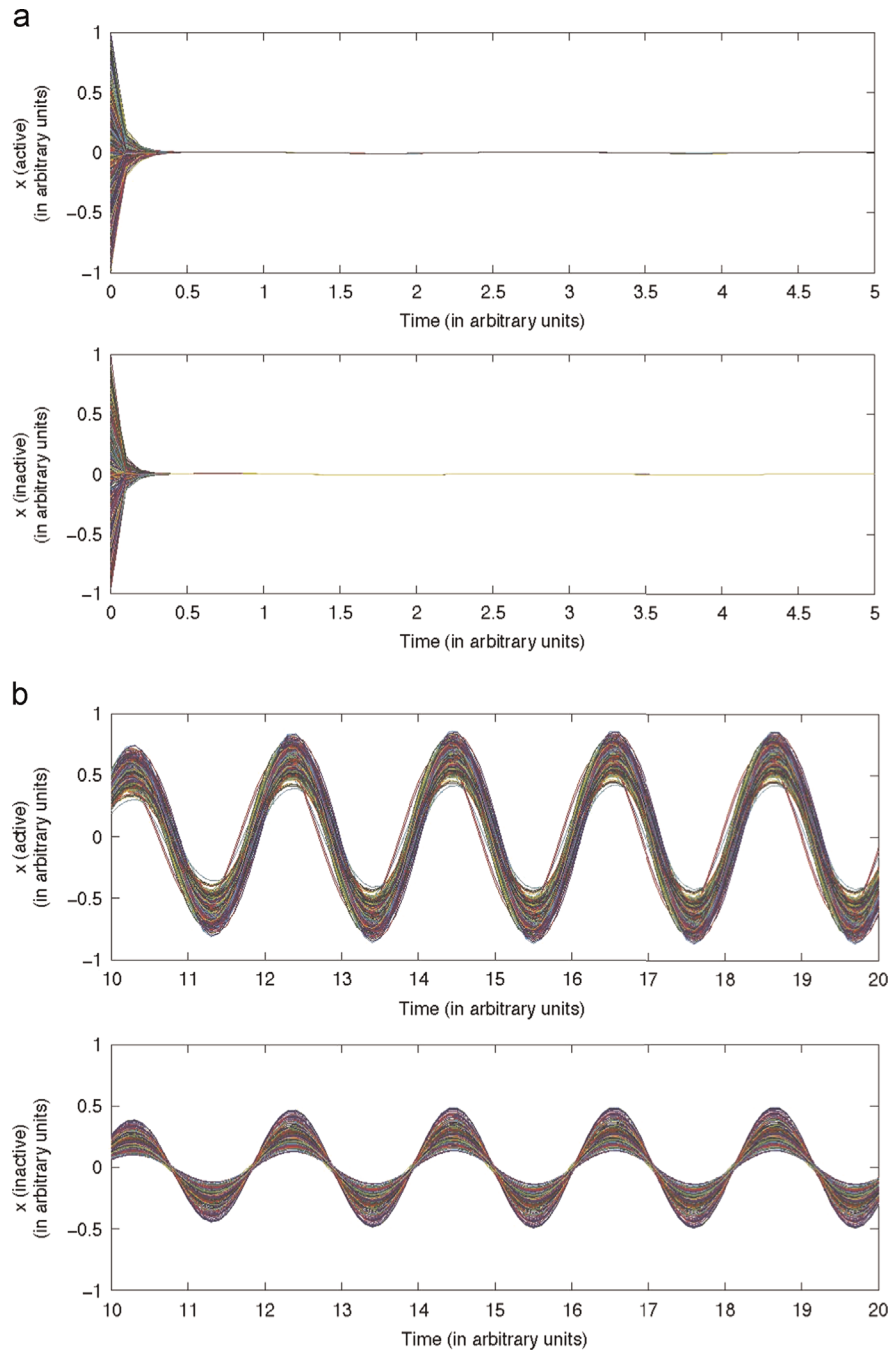

Fig. 9. State switching in a thousand Stuart–Landau oscillators coupled together using a power-law network topology. Of the thousand oscillators, growth rates (a_i) of 700 of them vary by 5% around a positive value of 1.0 (in the absence of coupling, these oscillators are active, that is, they oscillate); 300 of them vary by 5% around a negative value of -3.0 (in the absence of coupling, these oscillators are inactive, that is, they do not oscillate). The frequencies of the thousand oscillators (ω_i) vary by 5% around a value of 3.0. (A) System is in a steady state and no oscillations are present for $K=5$. Even the originally active oscillators (in the absence of coupling) become inactive so that the entire system exhibits steady state behavior. (B) System switches to an oscillatory state for $K=0.5$. Even the originally inactive oscillators (in the absence of coupling) become active so that the entire system exhibits oscillatory behavior.

could potentially "weigh in" to influence these decisions – by attenuating the pulsatile p53 response and overriding critical checkpoints, Myc can steer cell fate in yet another direction namely, cancer. A cancer cell can withstand severely damaged DNA (mutations, genetic lesions and chromosomal abnormalities are all hallmarks of cancer) yet is precluded from committing apoptosis because the p53 pulsatile response pathway is disabled.

Second, like numerous other oncogenes (Iakoucheva et al., 2002) and genes associated with cancer (Rajagopalan et al., 2011), Myc is an IDP. IDPs are proteins, or regions within proteins, that lack a stable tertiary structure in isolation but typically transition from disorder to order upon interaction with a partner (Tompa and Csermely, 2004). Despite the lack of structure, IDPs play important biological roles such as transcriptional regulation, chromatin remodeling and signaling (Iakoucheva et al., 2002; Sandhu, 2009). Because IDPs can populate multiple conformations they engage in myriad and often "promiscuous" interactions. These stochastic interactions between IDPs and their partners, defined as conformational noise, is an inherent characteristic of IDP interactions (Mahmoudabadi et al., 2013). The combined effect of conformational noise is an ensemble of protein network configurations, from which the most appropriate can be selected in response to perturbations. Thus, we had posited that noise due to IDP conformational dynamics could rewire protein networks and unmask latent interactions in response to perturbations to cause state-switching such as cellular transformation in cancer. Because numerous IDPs are found to be epigenetic modifiers and chromatin remodelers, we hypothesized that IDPs could further channel noise into stable, heritable genotypic changes (Mahmoudabadi et al., 2013). Thus, as an IDP, Myc could potentially, and promiscuously, affect the coupling constants of numerous other oscillators and rewire PINs to cause state switching. Finally, although we have focused on just two oscillators in this work to explain the Myc enigma, we have tested the feasibility of applying the model to a system with a thousand oscillators (Fig. 9) underscoring the potential of the model.

Biological systems, like many man-made systems built on the principles of engineering design, are self-organizing systems that are inherently robust to failure in an environment of uncertainty. A key determinant of robustness in the system is the presence of multiple feed forward and feedback loops (Cosentino and Bates, 2012). Thus, these nonlinear systems are often governed by oscillatory dynamics that play a critical for the system's behavior. For example, circadian rhythms (reviewed, (Bell-Pedersen et al., 2005)), the cell cycle (Goldbeter, 1991), and cell fate decision in response to DNA damage (reviewed, (Lahav, 2008)), are all governed by oscillatory dynamics of various cellular oscillators. Therefore, as illustrated in the present work, perturbations in the dynamics of key oscillators can have huge implications on cellular decisions. The proposed theoretical framework may not only help explain how Myc modulates state switching in cancer in the absence of differential gene expression or mutations, but may also be applicable in development and differentiation where Myc plays an important role. A detailed understanding of Myc regulatory circuitry could yield new insight into its functional dynamics and serve as a paradigm in deciphering the role of IDPs in cellular decision making.

Acknowledgments

Appendix A. Supplementary material

Supplementary data associated with this article can be found in the online version at http://dx.doi.org/10.1016/j.jtbi.2015.09.013.

References

Alam, M.J., Kumar, S., Singh, V., Singh, R.K., 2015. Bifurcation in cell cycle dynamics regulated by p53. PLoS One 10, e0129620.

Aylon, Y., Oren, M., 2007. Living with p53, dying of p53. Cell 130, 597–600.

Aronson, D.G., Doedel, E.J., Othmer, H.G., 1987. An analytical and numerical study of the bifurcations in a system of linearly coupled oscillators. Physica D 25, 20–104.

Aronson, D.G., Ermentrout, G.B., Kopell, N., 1990. Amplitude response of coupled oscillators. Physica D 41, 403–449.

Aguda, B.D., Kim, Y., Piper-Hunter, M.G., Friedman, A., Marsh, C.B., 2008. MicroRNA regulation of a cancer network: consequences of the feedback loops involving miR-17-92, E2F, and Myc. Proc. Natl. Acad. Sci. USA 105, 19678–19683.

Ben-Porath, I., Thomson, M.W., Carey, V.J., Ge, R., Bell, G.W., Regev, A., Weinberg, R. A., 2008. An embryonic stem cell-like gene expression signature in poorly differentiated aggressive human tumors. Nat. Genet. 40, 499–507.

Batchelor, E., Mock, C.S., Bhan, I., Loewer, A., Lahav, G., 2008. Recurrent initiation: a mechanism for triggering p53 pulses in response to DNA damage. Mol. Cell 30, 277–289.

Bell-Pedersen, D., Cassone, V.M., Earnest, D.J., Golden, S.S., Hardin, P.E., Thomas, T.L., Zoran, M.J., 2005. Circadian rhythms from multiple oscillators: lessons from diverse organisms. Nat. Rev. Genet. 6, 544–556.

Cole, M.D., Henriksson, M., 2006. 25 years of the c-Myc oncogene. Semin. Cancer Biol. 16, 241.

Chickarmane, V., Olariu, V., Peterson, C., 2012. Probing the role of stochasticity in a model of the embryonic stem cell: heterogeneous gene expression and reprogramming efficiency. BMC Syst. Biol. 6, 98–109.

Ciliberto, A., Novak, B., Tyson, J.J., 2005. Steady states and oscillations in the p53/Mdm2 network. Cell Cycle 4 (3), 488–493.

Cao, Z., Fan-Minogue, H., Bellovin, D.I., Yevtodiyenko, A., Arzeno, J., Yang, Q., Gambhir, S.S., Felsher, D.W., 2011. MYC phosphorylation, activation, and tumorigenic potential in hepatocellular carcinoma are regulated by HMG-CoA reductase. Cancer Res. 71, 2286–2297.

Csikasz-Nagy, A., Battogtokh, D., Chen, K.C., Novak, B., Tyson, J.J., 2006. Analysis of a generic model of eukaryotic cell-cycle regulation. Biophys. J. 90, 4361–4379.

Cosentino, C., Bates, D., 2012. Feedback Control in Systems Biology. CRC Press, New York.

Evans, T., Rosenthal, E.T., Youngblom, J., Distel, D., Hunt, T., 1983. Cyclin: a protein specified by maternal mRNA in sea urchin eggs that is destroyed at each cleavage division. Cell 33, 389–396.

Facchini, L.M., Penn, L.Z., 1998. The molecular role of Myc in growth and transformation: recent discoveries lead to new insights. FASEB J. 12, 633–651.

Felsher, D.W., Zetterberg, A., Zhu, J., Tlsty, T., Bishop, J.M., 2000. Overexpression of MYC causes p53-dependent G2 arrest of normal fibroblasts. Proc. Natl. Acad. Sci. USA 97, 10544–10548.

Felsher, D.W., Bishop, J.M., 1999. Reversible tumorigenesis by MYC in hematopoietic lineages. Mol. Cell 4, 199–207.

Fall, C.P., Marland, E.S., Wagner, J.M., Tyson, J.J. (Eds.), 2002. Computational Cell Biology. Springer-Verlag, New York, pp. 230–255.

Glauche, I., Herberg, M., Roeder, I., 2010. Nanog variability and pluripotency regulation of embryonic stem cells - insights from a mathematical model analysis. PLoS One 5, e11238.

Geva-Zatorsky, N., Rosenfeld, N., Itzkovitz, S., Milo, R., Sigal, A., Dekel, E., Yarnitzky, T., Liron, Y., Polak, P., Lahav, G., Alon, U., 2006. Oscillations and variability in the p53 system. Mol. Syst. Biol. 2 (2006), 0033.

Goldbeter, A., 1991. A minimal cascade model for the mitotic oscillator involving cyclin and cdc2 kinase. Proc. Natl. Acad. Sci. USA 88, 9107–9111.

Goldbeter, A., Gonze, D., Houart, G., Leloup, J.C., Halloy, J., Dupont, G., 2001. From simple to complex oscillatory behavior in metabolic and genetic control networks. Chaos 11, 247–260.

Gartel, A.L., Ye, X., Goufman, E., Shianov, P., Hay, N., Najmabadi, F., Tyner, A.L., 2001. Myc represses the p21(WAF1/CIP1) promoter and interacts with Sp1/Sp3. Proc. Natl. Acad. Sci. USA 98, 4510–4515.

Huang, H., Weng, H., Zhou, H., Qu, L., 2014. Attacking c-Myc: targeted and combined therapies for cancer. Curr. Pharm. Des. 20, 6543–6554.

Ho, J.S., Ma, W., Mao, D.Y., Benchimol, S., 2005. p53-Dependent transcriptional repression of c-myc is required for G1 cell cycle arrest. Mol. Cell Biol. 25, 7423–7431.

Hu, H., Du, L., Nagabayashi, G., Seeger, R.C., Gatti, R.A., 2010. ATM is down-regulated by N-Myc-regulated microRNA-421. Proc. Natl. Acad. Sci. USA 107, 1506–1511.

Iwakuma, T., Lozano, G., 2003. MDM2, an introduction. Mol. Cancer Res. 1, 993–1000.

Iakoucheva, L.M., Brown, C.J., Lawson, J.D., Obradović, Z., Dunker, A.K., 2002. Intrinsic disorder in cell-signaling and cancer-associated proteins. J. Mol. Biol. 323, 573–584.

Ji, H., Wu, G., Zhan, X., Nolan, A., Koh, C., De Marzo, A., Doan, H.M., Fan, J., Cheadle, C., Fallahi, M., Cleveland, J.L., Dang, C.V., Zeller, K.I., 2011. Cell-type independent MYC target genes reveal a primordial signature involved in biomass accumulation. PLoS One 6, e26057.

Johnson, D.G., Walker, C.L., 1999. Cyclins and cell cycle checkpoints. Annu. Rev. Pharmacol. Toxicol. 39, 295–312.

Kim, J., Orkin, S.H., 2011. Embryonic stem cell-specific signatures in cancer: insights into genomic regulatory networks and implications for medicine. Genome Med. 3, 75–82.

Kim, J., Woo, A.J., Chu, J., Snow, J.W., Fujiwara, Y., Kim, C.G., Cantor, A.B., Orkin, S.H., 2010. A Myc network accounts for similarities between embryonic stem and cancer cell transcription programs. Cell 143, 313–324.

Kalmar, T., Lim, C., Hayward, P., Muñoz-Descalzo, S., Nichols, J., Garcia-Ojalvo, J., Martinez Arias, A., 2009. Regulated fluctuations in nanog expression mediate cell fate decisions in embryonic stem cells. PLoS Biol. 7, e1000149.

Kim, J.K., Jackson, T.L., 2013. Mechanisms that enhance sustainability of p53 pulses. PLoS One 8 (6), e65242.

Kern, S.E., Kinzler, K.W., Bruskin, A., Jarosz, D., Friedman, P., Prives, C., Vogelstein, B., 1991. Identification of p53 as a sequence-specific DNA-binding protein. Science 252, 1708–1711.

Kuramoto, Y., 1984. Chemical Oscillations, Waves and Turbulence. Springer-Verlag, Berlin, pp. 8–13.

Lin, C.Y., Lovén, J., Rahl, P.B., Paranal, R.M., Burge, C.B., Bradner, J.E., Lee, T.I., Young, R.A., 2012. Transcriptional amplification in tumor cells with elevated c-Myc. Cell 151, 56–67.

Lee, J.H., Paull, T.T., 2007. Activation and regulation of ATM kinase activity in response to DNA double-strand breaks. Oncogene 26, 7741–7748.

Lahav, G., Rosenfeld, N., Sigal, A., Geva-Zatorsky, N., Levine, A.J., Elowitz, M.B., Alon, U., 2004. Dynamics of the p53-Mdm2 feedback loop in individual cells. Nat. Genet. 36, 147–150.

Levy, N., Yonish-Rouach, E., Oren, M., Kimchi, A., 1993. Complementation by wild-type p53 of interleukin-6 effects on M1 cells: induction of cell cycle exit and cooperativity with c-myc suppression. Mol. Cell Biol. 13, 7942–7952.

Liao, P., et al., 2014. A positive feedback loop between EBP2 and c-Myc regulates rDNA transcription, cell proliferation, and tumorigenesis. Cell Death Dis. 5, e1032.

Li, Y., Li, Y., Zhang, H., Chen, Y., 2011. MicroRNA-mediated positive feedback loop and optimized bistable switch in a cancer network Involving miR-17-92. PLoS One 6, e26302.

Lahav, G., 2008. Oscillations by the p53–Mdm2 feedback loop. In: Maroto, M., Monk, N.A.M. (Eds.), Cellular Oscillatory Mechanisms. Landes Bioscience, New York, pp. 28–38.

Marcu, K.B., Bossone, S.A., Patel, A.J., 1992. Myc function and regulation. Annu. Rev. Biochem. 61, 809–858.

Margolin, A.A., Palomero, T., Sumazin, P., Califano, A., Ferrando, A.A., Stolovitzky, G., 2009. ChIP-on-chip significance analysis reveals large-scale binding and regulation by human transcription factor oncogenes. Proc. Natl. Acad. Sci. USA 106, 244–249.

Maller, Jl, Gautier, J., Langan, T.A., Lohka, M.J., Shenoy, S., Shalloway, D., Nurse, P., 1989. Maturation-promoting factor and the regulation of the cell cycle. J. Cell Sci. Suppl. 12, 53–63.

Menssen, A., et al., 2012. The c-MYC oncoprotein, the NAMPT enzyme, the SIRT1-inhibitor DBC1, and the SIRT1 deacetylase form a positive feedback loop. Proc. Natl. Acad. Sci. USA 109, E187–E196.

Marshall, G.M., et al., 2011. SIRT1 promotes N-Myc oncogenesis through a positive feedback loop involving the effects of MKP3 and ERK on N-Myc protein stability. PLoS Genet. 7, e1002135.

Mahmoudabadi, G., Rajagopalan, K., Getzenberg, R.H., Hannenhalli, S., Rangarajan, G., Kulkarni, P., 2013. Intrinsically disordered proteins and conformational noise: implications in cancer. Cell Cycle 12, 26–31.

Nie, Z., Hu, G., Wei, G., Cui, K., Yamane, A., Resch, W., Wang, R., Green, D.R., Tessarollo, L., Casellas, R., Zhao, K., Levens, D., 2012. c-Myc is a universal amplifier of expressed genes in lymphocytes and embryonic stem cells. Cell 151, 68–79.

Ochs, R.S., 2014. Biochemistry. Jones & Bartlett Learning, Burlington.

Purvis, J.E., Karhohs, K.W., Mock, C., Batchelor, E., Loewer, A., Lahav, G., 2012. p53 dynamics control cell fate. Science 336 (6087), 1440–1444.

Rahl, P.B., Lin, C.Y., Seila, A.C., Flynn, R.A., McCuine, S., Burge, C.B., Sharp, P.A., Young, R.A., 2010. c-Myc regulates transcriptional pause release. Cell 141, 432–445.

Rajagopalan, K., Mooney, S.M., Parekh, N., Getzenberg, R.H., Kulkarni, P., 2011. A majority of the cancer/testis antigens are intrinsically disordered proteins. J. Cell Biochem. 112, 3256–3267.

Shaffer, A.L., Wright, G., Yang, L., Powell, J., Ngo, V., Lamy, L., Lam, L.T., Davis, R.E., Staudt, L.M., 2006. A library of gene expression signatures to illuminate normal and pathological lymphoid biology. Immunol. Rev. 210, 67–85.

Shachaf, C.M., Kopelman, A.M., Arvanitis, C., Karlsson, A., Beer, S., Mandl, S., Bachmann, M.H., Borowsky, A.D., Ruebner, B., Cardiff, R.D., Yang, Q., Bishop, J.M., Contag, C.H., Felsher, D.W., 2004. MYC inactivation uncovers pluripotent differentiation and tumour dormancy in hepatocellular cancer. Nature 431, 1112–1117.

Stratton, M.R., Campbell, P.J., Futreal, P.A., 2009. The cancer genome. Nature 458, 719–724.

Sun, T., Yang, W., Liu, J., Shen, P., 2011. Modeling the basal dynamics of p53 System. PLoS One 6, e27882.

Shiloh, Y., 2006. The ATM-mediated DNA-damage response: taking shape. Trends Biochem. Sci. 31, 402–410.

Shachaf, C.M., Gentles, A.J., Elchuri, S., Sahoo, D., Soen, Y., Sharpe, O., Perez, O.D., Chang, M., Mitchel, D., Robinson, W.H., Dill, D., Nolan, G.P., Plevritis, S.K., Felsher, D.W., 2008. Genomic and proteomic analysis reveals a threshold level of MYC required for tumor maintenance. Cancer Res. 68, 5132–5142.

Sachdeva, M., Zhu, S., Wu, F., Wu, H., Walia, V., Kumar, S., Elble, R., Watabe, K., Mo, Y.Y., 2009. p53 represses c-Myc through induction of the tumor suppressor miR-145. Proc. Natl. Acad. Sci. USA 106, 3207–3212.

Segel, L.A., Edelstein-Keshet, L., 2013. A Primer on Mathematical Models in Biology. SIAM, Philadelphia.

Slack, A., et al., 2005. The p53 regulatory gene MDM2 is a direct transcriptional target of MYCN in neuroblastoma. Proc. Natl. Acad. Sci. USA 102, 731–736.

Sandhu, K.S., 2009. Intrinsic disorder explains diverse nuclear roles of chromatin remodeling proteins. J. Mol. Recognit. 22, 1–8.

Takahashi, K., Yamanaka, S., 2006. Induction of pluripotent stem cells from mouse embryonic and adult fibroblast cultures by defined factors. Cell 126, 663–676.

Tompa, P., Csermely, P., 2004. The role of structural disorder in the function of RNA and protein chaperones. FASEB J. 18, 1169–1175.

Vogelstein, B., Kinzler, K.W., 2004. Cancer genes and the pathways they control. Nat. Med. 10, 789–799.

Vousden, K.H., Lane, D.P., 2007. p53 in health and disease. Nat. Rev. Mol. Cell Biol. 8, 275–283.

Wasylishen, A.R., Penn, L.Z., 2010. Myc: the beauty and the beast. Genes Cancer 1, 532–541.

Wagner, J., Ma, L., Rice, J.J., Hu, W., Levine, A.J., Stolovitzky, G.A., 2005. p53–Mdm2 loop controlled by a balance of its feedback strength and effective dampening using ATM and delayed feedback. IEE Proc. Syst. Biol. 152, 109–118.

Wang, X., Cunningham, M., Zhang, X., Tokarz, S., Laraway, B., Troxell, M., Sears, R.C., 2011. Phosphorylation regulates c-Myc's oncogenic activity in the mammary gland. Cancer Res. 71, 925–936.

Weis, M.C., Avva, J., Jacobberger, J.W., Sreenath, S.N., 2014. A data-driven, mathematical model of mammalian cell cycle regulation. PLoS One 9, e97130.

Zhang, X.P., Liu, F., Cheng, Z., Wang, W., 2009. Cell fate decision mediated by p53 pulses. Proc. Natl. Acad. Sci. USA 106, 12245–12250.